IOP Conf. Series: Materials Science and Engineering **160** (2016) 012041 doi:10.1088/1757-899X/160/1/012041

Numerical Study of a Winged Container Moving in an Air Tunnel

W M Shibani[1], M F Zulkafli[1], B Basuno[1]
[1] Department of Aeronautical Engineering, Faculty of Mechanical and Manufacturing Engineering, Universiti Tun Hussein Onn Malaysia 86400 Parit Raja, Johor, Malaysia

E-mail: wanismustafa@yahoo.com

Abstract. This study explores the movement of an object placed in an air tunnel. In expectation this exploration leads to obtaining a suitable shape of the object and the flow parameters, the object moves along the air tunnel has a particular trajectory. This study used the body of the main object is a cube in which a rectangular wing of aspect ratio 2 is set in the middle of body object. The object can be used as a carrier to transport goods from one place to another through an air tunnel. Three types wing-cube configurations, they are namely wing-cube configuration with airfoil sections (1) FX63-137, (2) NACA 4412, and (3) NACA 0012 are evaluated by using Fluent's software. The flow problems are treated as an internal flow problem with the assumption that the pressure ratio between the inlet and outlet of the air tunnel is 700 $\mathrm{N/m^2}$. The flow is treated as turbulent flow with $k-\varepsilon$ as its turbulence modelling. In this respect Fluent uses a SIMPLE scheme for solving their governing equation of fluid motion. Their computational results on the way the object moves along the air tunnel, it had been the carrier which uses airfoil NACA 0012 has better performance than the carrier that uses airfoil FX 63-137 or airfoil NACA 4412. This research work gives contribution in understanding the movement of the carrier in the form wing-cube configuration inside an air tunnel.

1. Introduction

Increasing human activities in the last two decades facilitated the significant growth of transportation of goods. Such a rapid increase in the demand for goods transport may seriously affect modern life. Present transportation systems, such as roads and railways, commonly involve route transportation. These transport systems involve problems such as traffic jams, accidents, air and noise pollutions, and damage to roads and bridges. These issues suggest the necessity of developing an alternative way of transporting goods from one place to another. Transportation through air tunnels may provide a solution to this problem. This approach will not interfere with the existing transportation system.

This study investigates a cubed container with attached wings. This carrier passes through an air tunnel. Wanis et al. [1] found that a cubed container that passes through an air tunnel has a fast-flying speed than a container with spherical or wedge shape. The plane form of the wing was rectangular. Three types of airfoils were chosen, namely, FX 63-137, NACA 0012, and NACA 4412.

As the problem becomes the flow problem of wing-body configuration, their aerodynamics characteristics are influenced by geometry parameter, such as aspect ratio, taper ratio, twist angle, wing incidence, the leading swept angle, etc. By adjusting the appropriate value for such wing parameter geometry one may obtain a suitable wing configuration to have a sufficient lift coefficient to make the container to flood. An extensive research in defining a suitable wing configuration mostly conducted in the aircraft manufacturer industries with the intention to get wing configuration has a higher maximum lift to drag ratio [2]. In addition to this, the flow problem under investigation belongs to the class of unsteady flow problems.

Fluent software version 16.1 is used to examine the movement of the carrier through an air tunnel. This software solves the governing equation of fluid motion in the form of time-averaged Navier-Stokes. Numerical schemes, such as SIMPLEC, SIMPLER, SIMPLEST, CTSSIMPLE, PISO, or SIMPLE, can be applied to solve this type of equation. Each of the numerical schemes has its own advantages and drawbacks [3–5]. Flow simulation that involves a Semi-Implicit Method for Pressure-Linked Equation (SIMPLE) scheme was used with time-averaged Navier-Stokes; the k − ε turbulence modeling proposed by Launder and Spalding was used in this scheme [6]. Song and Park [7] and Mohammadi and Pironneau [8] found that the k − ε model is accurate and robust. This model was also used by Chern and Wang [9] to investigate the flow rate of a ball valve. Gosman [10] showed the capability of this turbulence model to capture the turbulence during transport.

2. Description of the model

Figure 1 shows the cubed shape of carriers placed in an air tunnel. Wings are attached to the containers. The cube measures 0.1 m × 0.1 m × 0.1 m. Figure 2 shows that the wing has a chord length of 0.05 m and half of the wing is exposed. The wing placed in the middle of the cube has an incidence angle of 18°. The total mass of the carrier is 300 g.

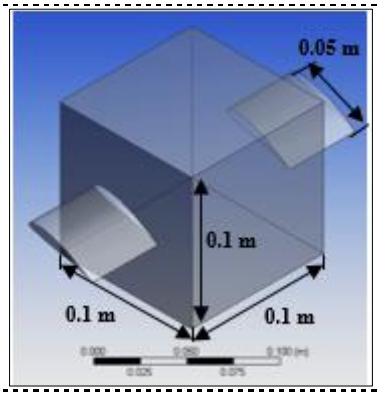

Figure 1. Rectangular carrier with wing for FX63-137 airfoil

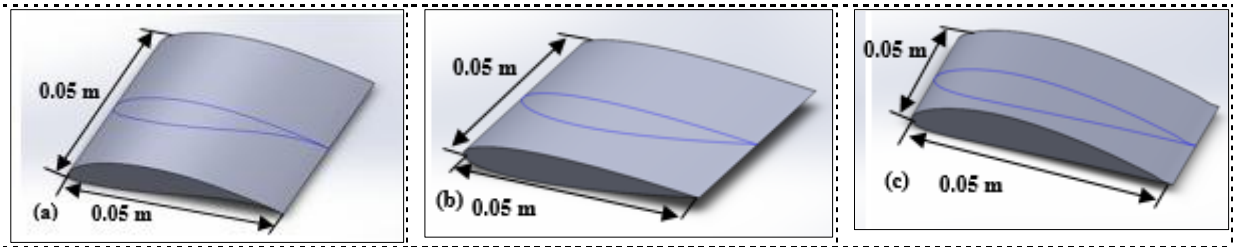

Figure 2. Rectangular wings for (a) FX63-137 airfoil, (b) NACA 0012 airfoil, and (c) NACA 4412 airfoil

Figure 3 shows that the air tunnel used in this study has a length of 5 m and a circular cross section with a diameter of 0.3 m.

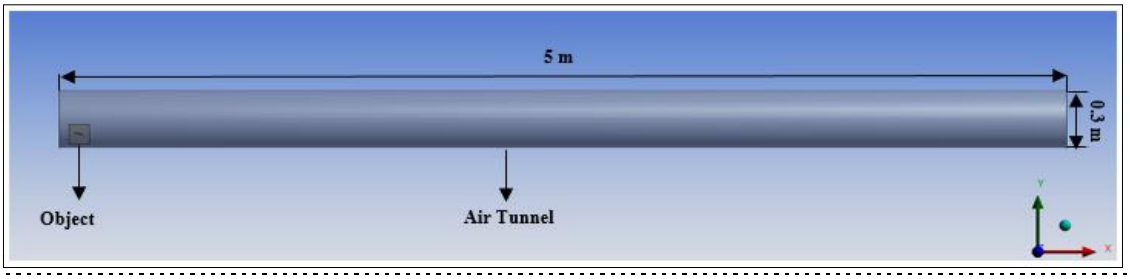

Figure 3. Dimensions of the 3D air tunnel

Figures 4 (a) and (b) show the initial position of the object in the air tunnel in the YZ- and XY-planes, respectively. The center of the object is set at the origin (0, 0, and 0). The distance of the center of the carrier's mass from the inlet of the air tunnel is 0.1 m. Distance from the lower wall of the air tunnel is 0.07 m and 0.23 m from the upper wall.

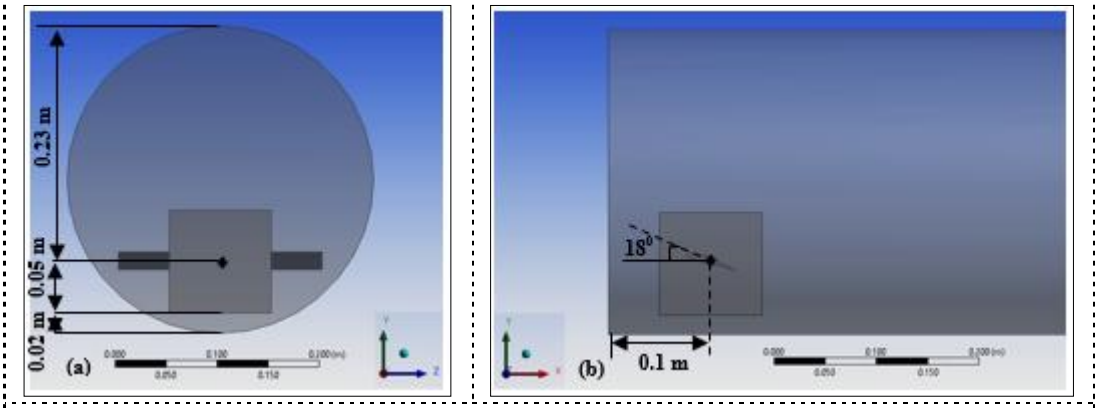

Figure 4. Air tunnel (a) YZ plane, and (b) XY plane

3. Mesh topologies

The carriers were prepared using SOLIDWORKS software [11] and later imported into the ANSYS software [12]. A non-uniform unstructured mesh was used with a considerable fine mesh implemented in the regions of high gradients. A tetrahedron element was selected as the mesh of the carriers and air tunnel. Tetrahedron mesh is rarely used in wind engineering literature because of its lower efficiency in space discretization than structured mesh [13]. The advantage of tetrahedral mesh is its flexibility. Figure 5 shows the layout of the cross-sectional plane of the mesh. The number of mesh grids ranged from 2167512 to 2928238.

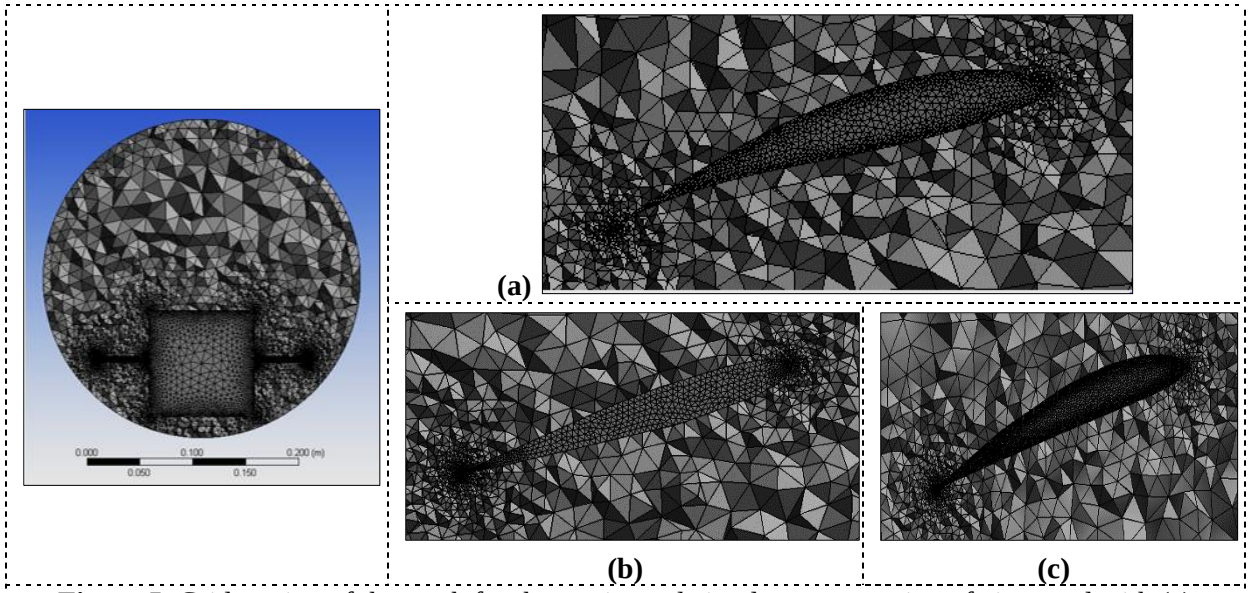

Figure 5. Grid section of the mesh for the carrier and circular cross-section of air tunnel with (a) FX63-137 airfoil, (b) NACA 0012 airfoil, and (c) NACA 4412 airfoil

4. Numerical calculation method

In the use of FLUENT software version 16.1 [12], present work use option a SIMPLE scheme for its flow solver and the $k-\varepsilon$ turbulence model as its turbulence modelling. Such approach had been applied to study the object movement along the air tunnel as presented in Ref. [14].

4.1. Governing equations

Flow problems are treated as three-dimensional incompressible flow problems because of the low flow speed at the inlet station at around 33 m/s. Assuming that temperature variation does not exist in the tunnel, the incompressible time-averaged Navier–Stokes equation solved by FLUENT may take the following form which is in tensor form [15]:

$$\nabla . u = 0 \tag{1}$$

$$\rho \frac{D\overline{u_i}}{D_t} = F_i - \frac{\partial \bar{p}}{\partial x_i} + \mu \Delta \overline{u_i} - \rho \left(\frac{\partial \overline{u_i' u_j'}}{\partial x_j} \right) \tag{2}$$

where ρ denotes density; F is force, μ is molecular viscosity, Δ is vector operator, ū is time-averaged velocity components, $\bar{p}$ is time-averaged pressure, and u' is fluctuating velocity components and index i, j denotes the spatial dimension index.

4.2. Boundary Conditions

The physical boundary condition of these problems are as follows:

1) Each end of the air tunnel is considered pressure inlet and outlet, whereas the surface of the moving carriers and the air tunnel is considered the wall, i.e., no-slip boundary condition $u = v = w = 0$. (See Figure 6).
2) "Pressure inlet" was constantly set to 700 N/m^2 higher than the atmospheric pressure. This level is equivalent to the velocity of 33 m/s at the boundary condition of the inlet.
3) The right surface of the computational domain is assigned as the outlet. The boundary condition for "pressure outlet" is implemented at the exit boundary with the zero input value of the static gauge pressure, i.e., $\frac{\partial u}{\partial x} = \frac{\partial v}{\partial x} = \frac{\partial w}{\partial x} = 0$ of the Dirichlet-type pressure boundary condition.

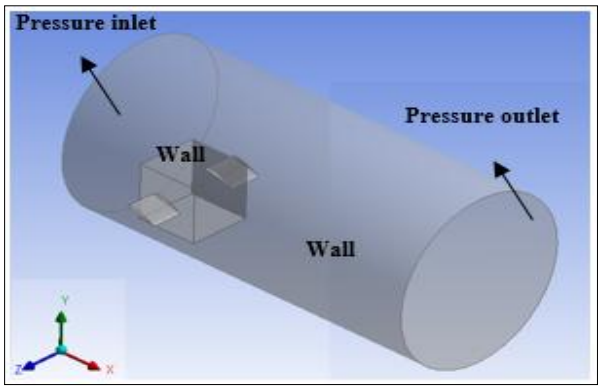

Figure 6. Boundary conditions of the air tunnel and carrier

5. Calculation results and analysis

The movement of the carriers in time was tracked according to the movement of the center of gravity of the carrier. Figures 7 to 9 show the plot of the center of gravity of the location in the x, y, and z directions with respect to time. These graphs also plot the polynomial functions.

Thev_x,v_y and v_z velocity components can be determined by obtaining the first derivative with time to the corresponding polynomial function. The total velocity v_c of each carrier can be obtained as:

$$v_c = \sqrt[2]{\left(v_x^2 + v_y^2 + v_z^2\right)}. \quad (4)$$

The comparison total velocity v_c for these three model carriers are shown in Figure 10.

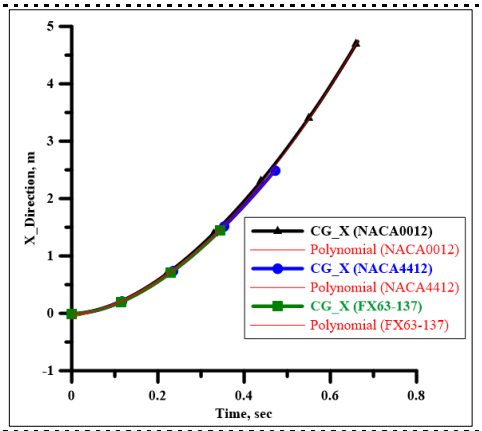

Figure 7. Distance in x-direction for all carriers

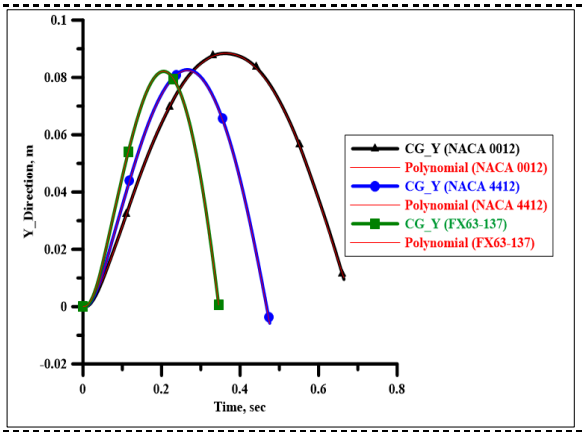

Figure 8. Distance in y-direction for all carriers

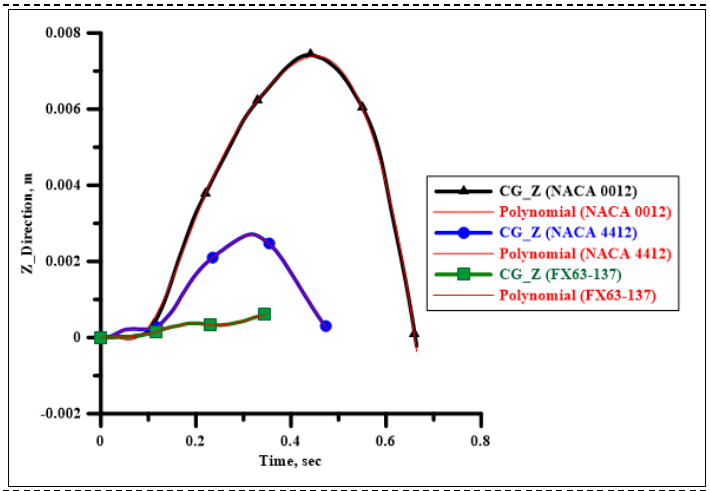

Figure 9. Distance in z-direction for all carriers

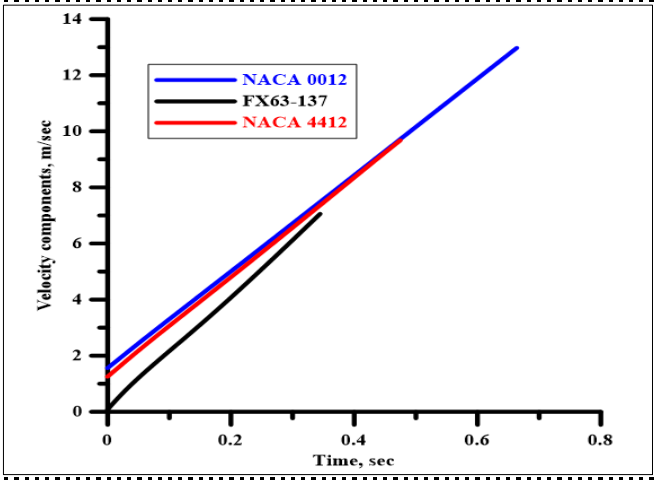

Figure 10. Velocity component for the carriers with respect to time

Figure 8 shows that the carrier of FX63-137 raised to 0.082 m in the Y-direction, which is the highest point in the graph at 0.21 s. However, the highest point at the beginning covered the short distance along the air tunnel because of the force acting on the carrier during the launching time. This finding is attributed to the different distances covered by the carriers.

Figure 9 shows that the shortest distance covered by the FX63-137 carrier showed the better stability of moving in Z-direction than other carriers.

Figure 10 shows that the carrier with airfoil section NACA 0012 begins with the speed of 1.56 m/s and reached the speed of 12.98 m/s at time t = 0.663 s with an achievable distance of 4.74 m. This carrier model has the highest speed and the longest distance among the three carrier models.

The flow pattern that surrounds the carriers at different stations is shown by the contours of pressure. The front view is shown in Figures 11, 13, and 15, whereas the side view is illustrated in Figures 12, 14, and 16 for further clarifications of the movement. These figures describe the flow conditions at various time steps.

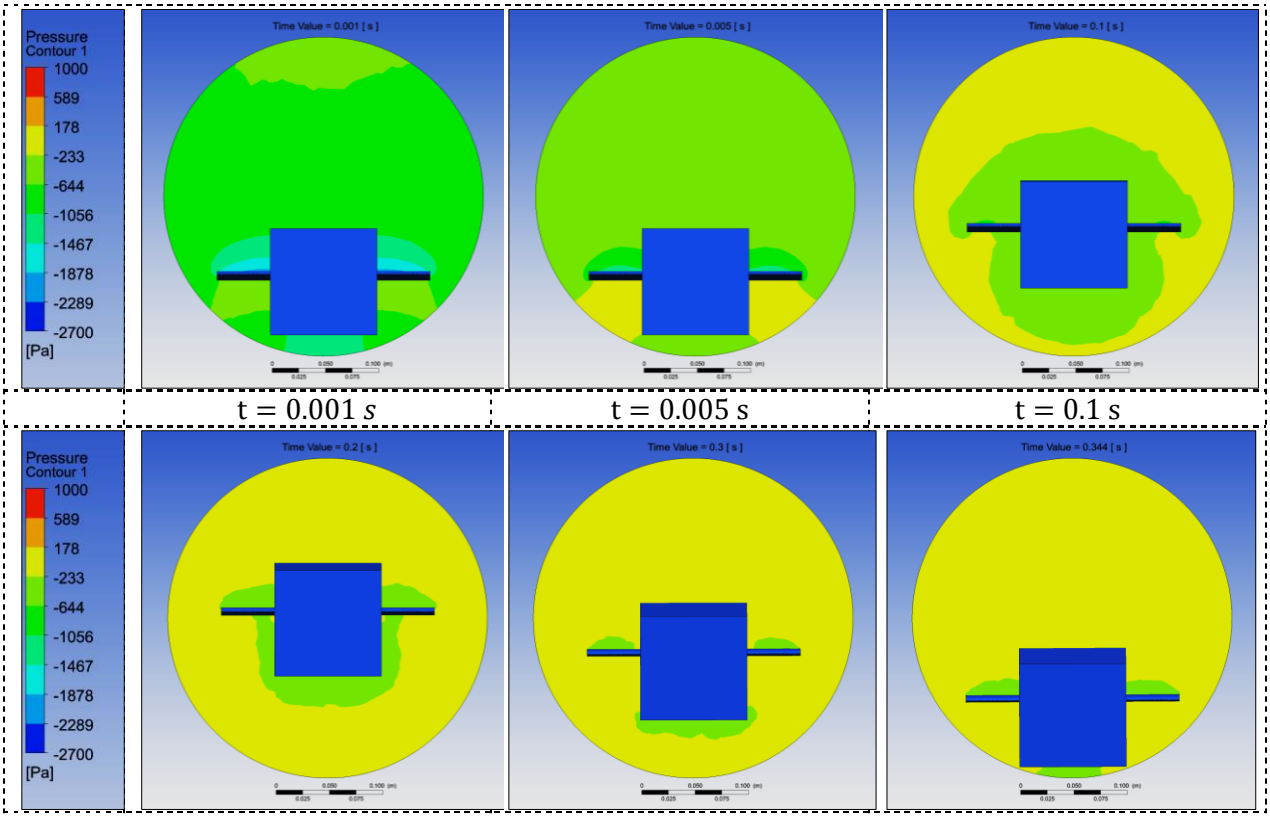

Figure 11. Pressure contours of the flow field around the carrier in various positions in the X-direction and YZ-plane for the case of airfoil wing section FX63-137

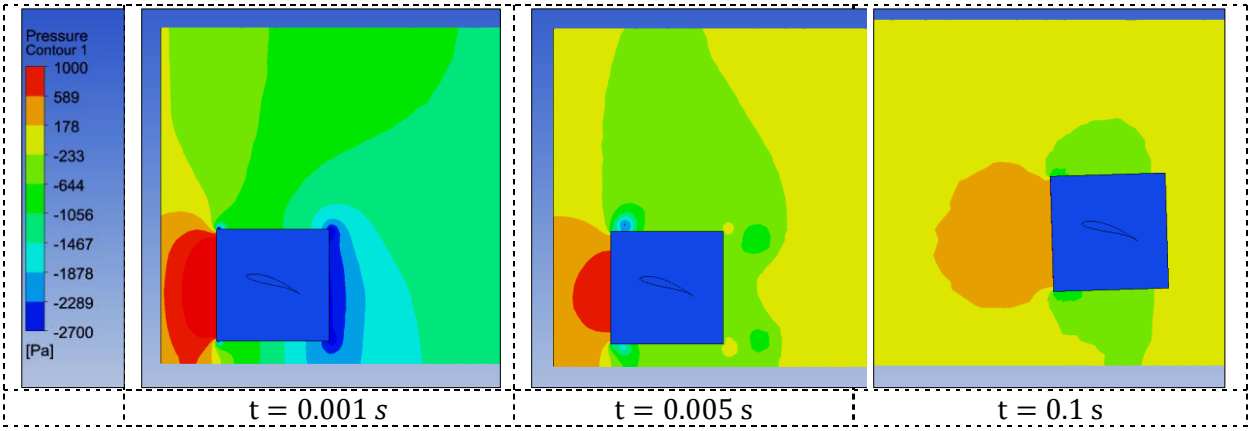

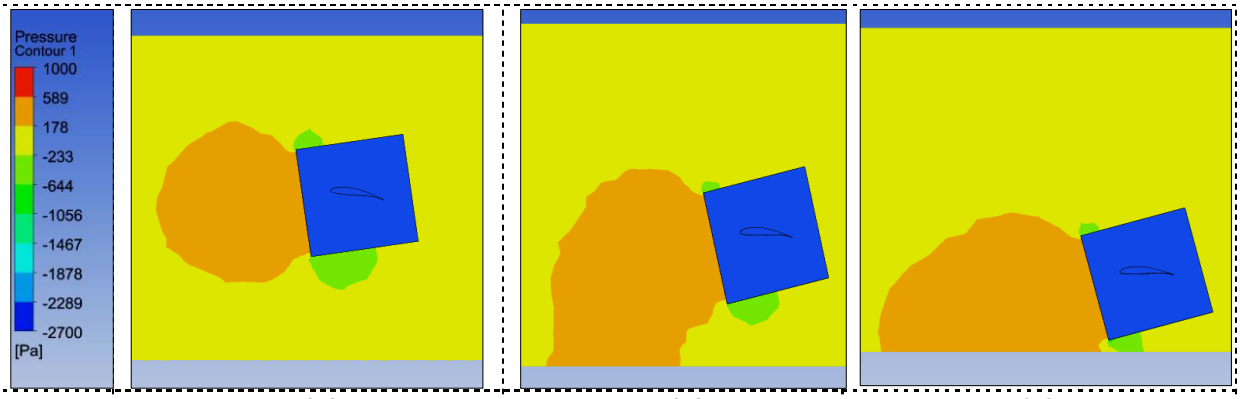

t = 0.2 *s* | t = 0.3 s | t = 0.344 s

Figure 12. Pressure contours for the flow field around the carrier in various positions in the X-direction and YX-plane for the case of airfoil wing section FX63-137

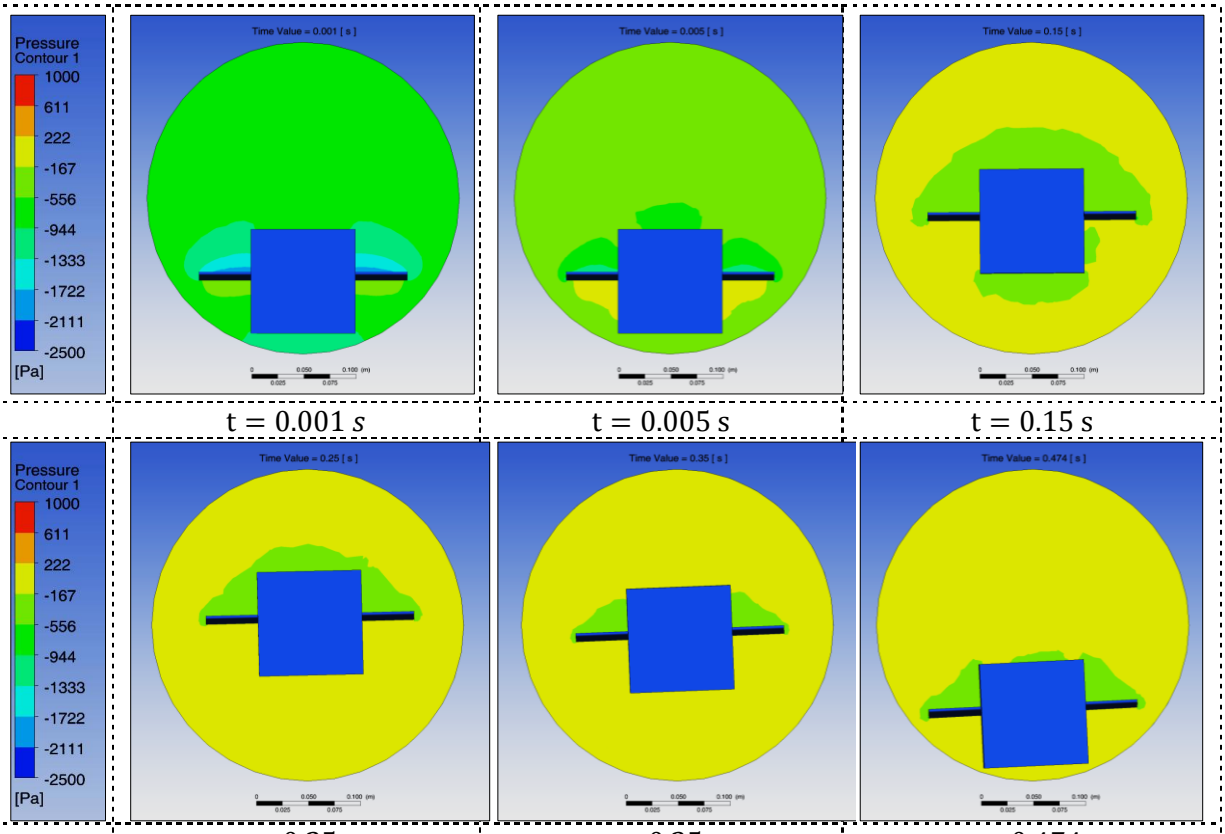

t = 0.001 *s* | t = 0.005 s | t = 0.15 s

t = 0.25 *s* | t = 0.35 s | t = 0.474 s

Figure 13. Pressure contours of the flow field around the carrier in various positions in the X-direction and YZ-plane for the case of airfoil wing section NACA 4412

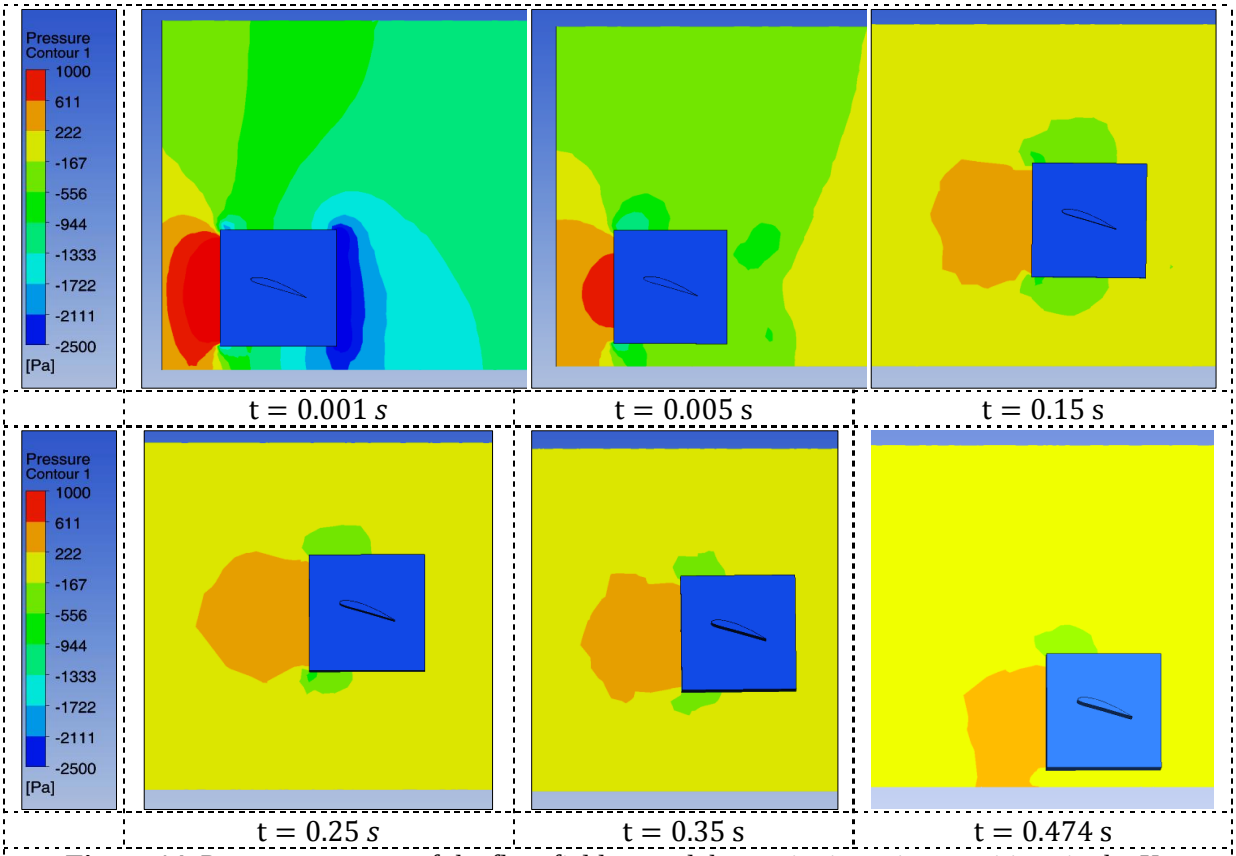

Figure 14. Pressure contours of the flow field around the carrier in various positions in the X-direction and YZ-plane for the case of airfoil wing section NACA 4412

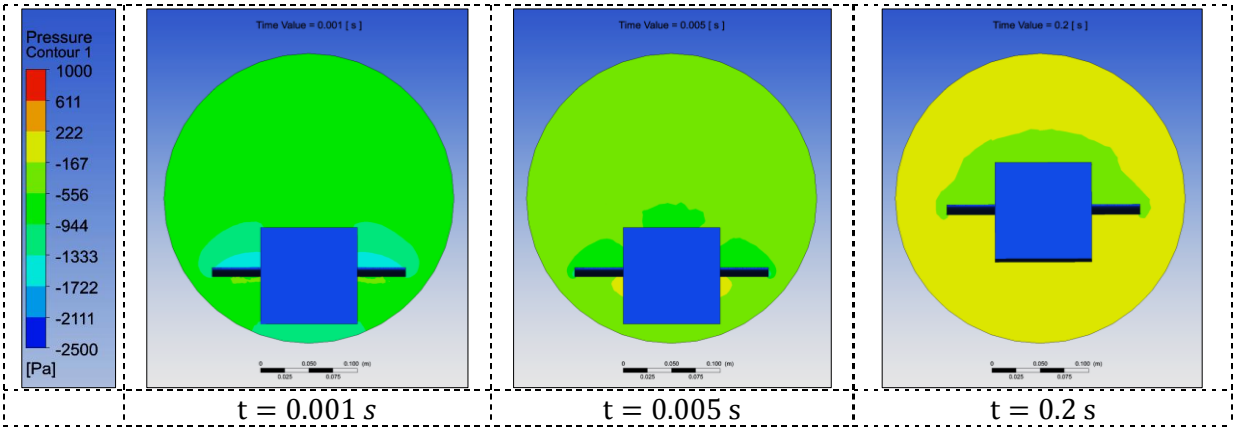

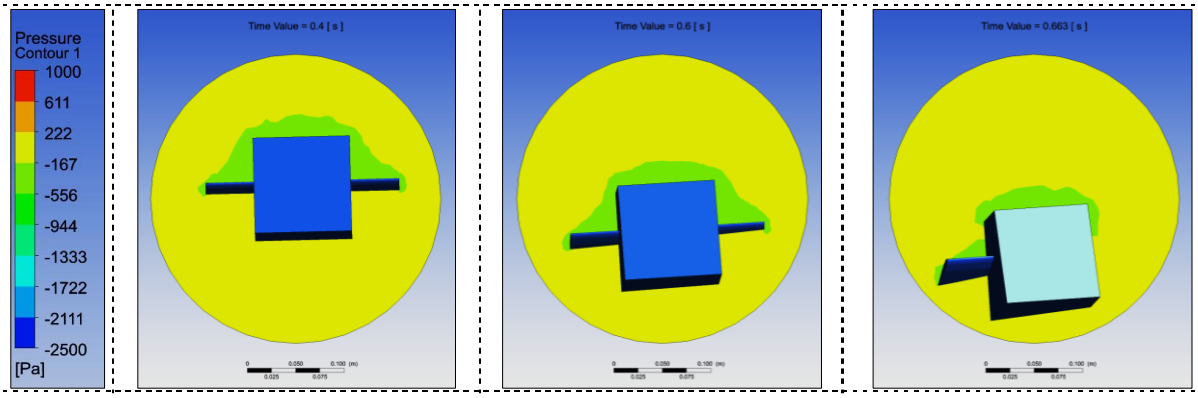

Figure 15. Pressure contours of the flow field around the carrier in various positions in the X-direction and YZ-plane for the case of airfoil wing section NACA 0012

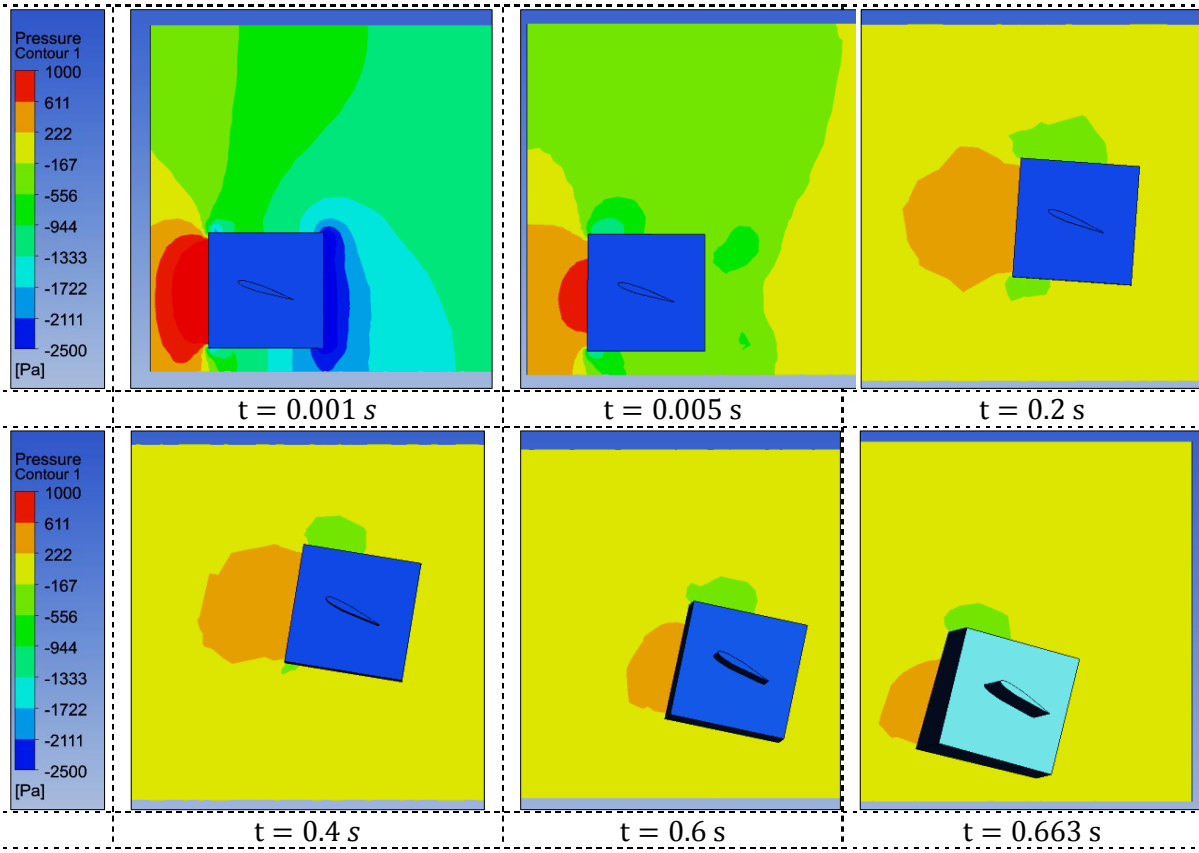

Figure 16. Pressure contours of the flow field around the carrier in various positions in the X-direction and YZ-plane for the case of airfoil wing section NACA 0012

Figure 17 shows the results obtained from FLUENT analysis by tracking the carriers using the center of gravity in the XY-plane along the air tunnel.

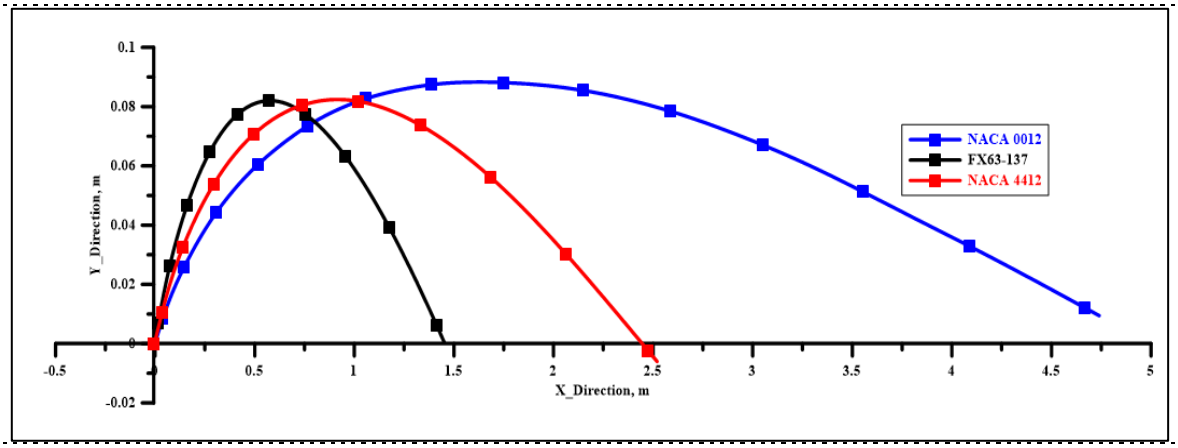

Figure 17. Carrier trajectory with characteristic squares

The results are shown in Figures 11 to 17 give this description:

- The carrier (FX63-137) moves with a speed of 0.09 m/s at the beginning of the motion at 0.001 s (see Figures 10 and 11) and the lift force works on the carrier is 5.05 N. While, the carrier (NACA 4412) moves with a speed of 1.25 m/s at the beginning of the motion at 0.001 s (see Figures 13 and 14) and the overall lift force work on it is 3.83 N. Also the carrier (NACA 0012) moves at a speed of 1.56 m/s in the beginning of the motion at 0.001 s (see Figures 14 and 15) with the overall lift force work on the carrier is 3.14 N.
- As time progresses, the speed of the carrier (FX63-137) rapidly increases to achieve the speed of 7.06 m/s and make the carrier moves to a distance of 1.45 m in the X-direction at 0.344 s. While the carrier (NACA 4412) has a speed increment to the speed of 9.68 m/s and allow the carrier moves to a distance of 2.52 m in the X-direction at 0.474 s. While the speed of the carrier (NACA 0012) rapidly increases to achieve the speed of 12.98 m/s and allow the carrier to move a distance of 4.74 m in the X-direction at 0.663 s.

From above results indicates the carrier NACA 0012 can move faster and achieve a longer distance compared to two other carriers. This is due to the fact during the movement of the carrier NACA 0012, the pitching moment, creating by the wing relatively a low, so the body rotates slowly and need more time to stall. If during the carrier floats, if it can be introduced, some mechanism to set the pitching moment coefficients work on that carrier to zero, the ability of the carrier to float for a long distance may achievable.

These results indicate the possibility of moving or transporting carriers through air tunnels. Increased distance can be achieved if the angle of the wing with respect to the horizontal line is adjusted to zero maintain pitching moment on the carrier. The carrier floats with a lift equal to the carrier weight. Rotation does not exist in this situation.

6. Conclusion

A numerical study of three-dimensional unsteady flow problems was performed. Three cube-shaped carriers were examined. The wings were attached to the containers. The motions of the three carriers in the air tunnel were compared. The pressure contours of the flow field are presented with 3D flow problems. The numerical simulations indicate that there is possibly a particular carrier's configuration to be used as a container for transporting goods through air tunnel. The distance covered by the carrier (NACA 0012) is 4.74 m, which is 95% of the length of air tunnel and is longer than the distance achieved by NACA 4412 and FX63-137. The distances achieved by NACA 4412 and FX63-137 respectively cover 50% and 29% of the air tunnel length.

Acknowledgment
The authors thank Universiti Tun Hussein Onn Malaysia (Grant Code: U416) for providing financial support for this research.

7. References

[1] Shibani W, Zulkafli F, and Basuno B. A comparative study on the motion of various objects inside an air tunnel. paper presented at the 7th *International conference on Mechanical and Manufacturing Engineering (ICME2016)*, Jogjakarta city (Indonesia), 01-03 August, accepted on 14th July 2016**.**

[2] Hossain A, Rahman A, Iqbal AK, Ariffin M, Mazian M. Drag analysis of an aircraft wing model with and without bird feather like winglet. *International Journal of Aerospace and Mechanical Engineering.* 2012;6(1):**8-13**.

[3] Tao WQ. Numerical heat transfer *Xi'an Jiaotong University. Xi'an*. 2001:**362-70**.

[4] Zhaoshun Z, Guixiang C, and Chunxiao X. Approaching to turbulence. *Mechanics in Engineering*. 2002;24(1):**1-8**.

[5] Sohankar A, Davidson L, and Norberg C. Numerical simulation of unsteady flow around a square two-dimensional cylinder. *In Proc. 12-th Australasian Fluid Mechanics Conference* 1995 Dec (**pp. 517-520**).

[6] Launder BE and Sharma BI. Application of the energy-dissipation model of turbulence to the calculation of flow near a spinning disc. *Letters in heat and mass transfer*. 1974 Nov 1;1(2):**131-7**.

[7] Guan Song X and Park YC. Numerical analysis of butterfly valve-prediction of flow coefficient and hydrodynamic torque coefficient. *In Proceedings of the world congress on Engineering and computer science* 2007 (**pp. 24-26**).

[8] Mohammadi B. Analysis of the K-Epsilon Turbulence Model. *Applied Mechanics Reviews*. 1994;47(12): **B117**.

[9] Chern MJ and Wang CC. Control of volumetric flow-rate of ball valve using V-port. *Journal of fluids engineering*. 2004 May 1;126(3):**471-81**.

[10] Gosman AD. Developments in CFD for industrial and environmental applications in wind engineering. *Journal of Wind Engineering and Industrial Aerodynamics*. 1999 May 31;81(1):**21-39**.

[11] Tickoo S. *SolidWorks for designers* (Schererville, IN, USA): release 2016, 14th Edition. Cadcim Technologies; 2016.

[12] Fluent, ANSYS. *ANSYS Fluent User's Guide*, (Canonsburg, PA, USA, 2015) release 16.2: **1-2718**.

[13] Yu Y, Barron RM and Balachandar R. Numerical Prediction of Pressure Distribution on a Cube Obstacle in Atmospheric Boundary Layer Flow.

[14] Shibani E, Zulkafli MF, Basuno B and Ab Wahab AB. Numerical Analysis of a Moving Object in the Air Tunnel. *International Journal of Mechanical & Mechatronics Engineering IJMME*. 2016;16(03):**72-8**.

[15] Masatsuka K. *I Do Like CFD*, Vol. 1. Lulu. com; 2013.